

S. Speziale · T. S. Duffy

Single-crystal elastic constants of fluorite (CaF₂) to 9.3 GPa

Received: 10 July 2001 / Accepted: 7 March 2002

Abstract The second-order elastic constants of CaF₂ (fluorite) have been determined by Brillouin scattering to 9.3 GPa at 300 K. Acoustic velocities have been measured in the (111) plane and inverted to simultaneously obtain the elastic constants and the orientation of the crystal. A notable feature of the present inversion is that only the density at ambient condition was used in the inversion. We obtain high-pressure densities directly from Brillouin data by conversion to isothermal conditions and iterative integration of the compression curve. The pressure derivative of the isentropic bulk modulus and of the shear modulus determined in this study are 4.78 ± 0.13 and 1.08 ± 0.07 , which differ from previous low-pressure ultrasonic elasticity measurements. The pressure derivative of the isothermal bulk modulus is 4.83 ± 0.13 , 8% lower than the value from static compression, and its uncertainty is lower by a factor of 3. The elastic constants of fluorite increase almost linearly with pressure over the whole investigated pressure range. However, at $P \geq 9$ GPa, C_{11} and C_{12} show a subtle structure in their pressure dependence while C_{44} does not. The behavior of the elastic constants of fluorite in the 9–9.3 GPa pressure range is probably affected by the onset of a high-pressure structural transition to a lower symmetry phase (α -PbCl₂ type). A single-crystal Raman scattering experiment performed in parallel to the Brillouin measurements shows the appearance of new features at 8.7 GPa. The new features are continuously observed to 49.2 GPa, confirming that the orthorhombic high-pressure phase is stable along the whole investigated pressure range, in agreement with a previous X-ray diffraction study of CaF₂ to 45 GPa. The high-pressure elasticity data in combination with room-pressure values from previous studies allowed us to determine an independent room-temperature compression

curve of fluorite. The new compression curve yields a maximum discrepancy of 0.05 GPa at 9.5 GPa with respect to that derived from static compression by Angel (1993). This comparison suggests that the accuracy of the fluorite pressure scale is better than 1% over the 0–9 GPa pressure range.

Keywords Brillouin scattering · Single-crystal elastic constants · Raman scattering

Introduction

Fluorite, the ambient pressure polymorph of CaF₂, is a simple alkali halide, and represents a model ionic solid in solid-state physics. It has cubic symmetry ($Fm\bar{3}m$) and is the prototype of an important structure type for metal halides, binary sulfides, and metallic alloys. On the basis of X-ray diffraction, CaF₂ was observed to undergo a structural phase transition to the orthorhombic PbCl₂ type structure ($Pbmn$), at 9.5 GPa. The high-pressure phase was shown to be stable to 45 GPa at 300 K by X-ray diffraction (Gerward et al. 1992).

Fluorite is, in many respects, an ideal material to serve as a pressure calibrant in moderate high-pressure/high-temperature X-ray diffraction experiments (Hazen and Finger 1981; Katrusiak and Nelmes 1986; Angel 1993; Angel et al. 1997; Miletich et al. 2001). The use of internal diffraction standards of known equation of state is the method of choice for high-precision pressure determination in high-pressure crystallographic studies (Miletich et al. 2001). Recently, it was shown that the achievable precision of volume determination of quartz single crystals to 9 GPa allows for pressure precisions as high as 0.05–0.1% (Angel et al. 1997).

Unfortunately, the accuracy of the pressure determination is not as well constrained. In fact, the very high precision measurements of quartz depend on the equation of state of fluorite, which was used as internal pressure standard in that study. The equation of state of CaF₂, based on single-crystal X-ray data and the ruby fluorescence scale, has been determined to 9.5 GPa

S. Speziale (✉) · T. S. Duffy
Department of Geosciences, Princeton University,
Princeton New Jersey, 08544 USA
e-mail: speziale@Princeton.EDU
Tel.: 001-609-258-3261; Fax: 001-609-258-1274

(Angel 1993). In this study we provide an independent test of the equation of state parameters of fluorite using high-pressure Brillouin scattering.

The elasticity of CaF₂ has been investigated by ultrasonic interferometry to pressure only as high as 1.2 GPa at low temperature (4.2 to 298 K; Ho and Ruoff 1967; Wong and Schuele 1968; Brielles and Vidal 1975) and at ambient pressure to 1125 K (Vidal 1974; Jones 1977), and by Brillouin spectroscopy to 1500 K at ambient pressure (Catlow et al. 1978). There are significant discrepancies between the pressure derivatives of the individual constants and the aggregate moduli (Tables 1, 2). Recently, theoretical simulations of CaF₂ (Catti et al. 1991; Martín-Pendás et al. 1994) have furnished additional information about high-pressure elastic properties. The present study was designed to resolve the discrepancies in the pressure dependencies of the elastic moduli of fluorite.

The high-pressure phase transition of CaF₂ has been reported in several X-ray studies (Seifert 1966; Dandekar and Jamieson 1969; Gerward et al. 1992), but the quality of the metastably recovered high-pressure phase does not allow a single-crystal structure refinement. Only recently, a crystal structure refinement was performed on a pressure- and temperature-quenched single crystal, grown at 8.6 GPa and 1100 K in a molten Ca(OH)₂ flux (Morris et al. 2001). Our Brillouin scattering investigation has been supplemented by Raman measurements of polycrystalline powder and of single-crystal plates to 49.2 GPa in order to correlate possible elastic anomalies to the onset of the structural transition to the high-pressure phase and to explore the stability of the high-pressure polymorph of CaF₂. In fact, it is expected that the orthorhombic phase may eventually transform to a hexagonal Ni₂In structure type in analogy to the transition observed in BaF₂ at 12 GPa and 300 K (Legér et al. 1995).

Experimental technique

Brillouin scattering measurements

A natural colorless fluorite crystal of unknown origin was cut and polished to a 20- μ m-thick plate parallel to the (111) crystallographic plane. The lattice constant at atmospheric pressure had been determined by powder X-ray diffraction on the same material to be 5.4631 ± 0.0004 , in good agreement with the value of 5.4632 ± 0.0003 measured by Hazen and Finger (1981). The sample was loaded in a modified Merrill-Basset cell (Merrill and Bassett 1974) with a 96° aperture angle. A cylindrical sample chamber was obtained by machining a 250- μ m-diameter hole in a stainless steel gasket preindented to a thickness of 50- μ m. The sample was compressed between 500- μ m diamond culets, and either a 4:1 volume mixture of methanol and ethanol or silicone grease was used as a pressure-transmitting medium. Ruby chips were used as pressure markers (Barnett et al. 1973; Mao et al. 1986) and to check the pressure distribution in the sample chamber by analyzing the sharpness of the ruby peaks (Chai and Brown 1996). The variation of the width of the ruby peak at different positions and at the different pressures never exceeded 15% of the width registered at ambient pressure, in agreement with previous tests in high-pressure Brillouin experiments (Sinogeikin and Bass 2000). Pressure differences between grains at different positions in the sample chamber never exceeded ± 0.2 GPa.

Brillouin scattering experiments were performed in a forward symmetric geometry, which allows determination of the acoustic velocity independent of the refractive index of the sample (Withfield et al. 1976). The Brillouin effect was excited using 160 mW of a vertically polarized neodymium vanadate laser ($\lambda = 532.15$ nm), measured using a six-pass Sandercock tandem Fabry-Perot interferometer (Lindsay et al. 1981), and recorded by a solid-state photon detector with 70% quantum efficiency in the frequency range of interest. A diagram of the setup of our Brillouin system is shown in Fig. 1.

In the forward symmetric scattering geometry, the Brillouin frequency shift, $\Delta\nu$, is related to the acoustic velocity, v , through the relation:

$$v = \frac{\Delta\nu\lambda_0}{2 \sin \alpha}, \quad (1)$$

Table 1 Elastic constants of CaF₂, and their pressure derivatives at ambient conditions. Numbers in parentheses are one standard deviation uncertainty in the last digits

| Study | C_{11} (GPa) | C_{12} (GPa) | C_{44} (GPa) | $(\partial C_{11}/\partial P)_T$ | $(\partial C_{12}/\partial P)_T$ | $(\partial C_{44}/\partial P)_T$ |
|--|----------------|----------------|----------------|----------------------------------|----------------------------------|----------------------------------|
| This study ^a | 165.5 (9) | 44.4 (5) | 34.2 (3) | 5.99 (15) | 4.25 (9) | 1.15 (4) |
| Ultrasonic interferometry ^b | | | | | | |
| H | 163.6 | 44.0 | 33.9 | | | |
| H-R | 165.07 (6) | 44.51 (5) | 33.83 (5) | 6.62 (37) | 6.08 (28) | 1.33 (4) |
| W-S | 164.2 | 43.98 | 33.7 | 6.05 | 4.35 | 1.31 |
| B-V | 165.2 | 45.4 | 33.7 | 5.74 | 4.2 | 1.29 |
| J | 165.1 (3) | 44.3 (4) | 33.85 (6) | | | |
| Average | 164.6 (7) | 44.4 (6) | 33.8 (1) | | | |
| Brillouin spectroscopy | | | | | | |
| C | 166 (3) | 39 (3) | 34 (2) | | | |
| Theory ^c | | | | | | |
| Ca | 172.2 | 38.6 | 44 | | | |
| MP | 171.4 | 38.3 | | 4.6 | 3.8 | |

^a C_{11} , C_{12} , C_{44} and their pressure derivatives are from finite strain fits incorporating high-pressure data together with average values of the elastic constants at ambient conditions from ultrasonic interferometry

^b Previous studies: *H* Haussühl (1963); *H-R* Ho and Ruoff (1967); *W-S* Wong and Schuele (1968); *B-V* Brielles and Vidal (1975);

J Jones (1977); *C* Catlow et al. (1978); *Ca* Catti et al. (1991); *MP* Martín-Pendás et al. (1994)

^c Athermal parameters

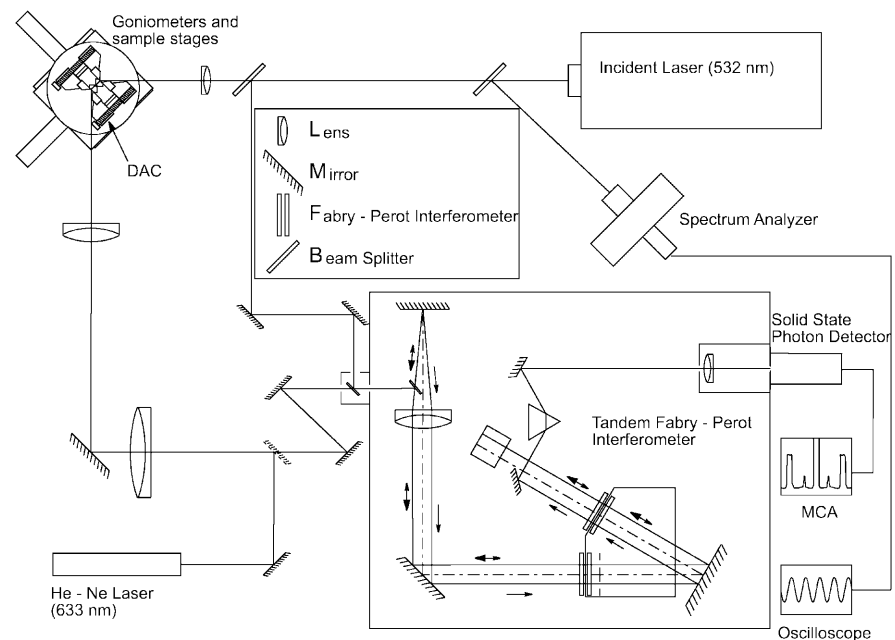
Table 2 Hill average of the Reuss and Voigt aggregate bulk and shear moduli of CaF₂, and their pressure derivatives under ambient conditions. Numbers in parentheses are one standard deviation uncertainty in the last digits

| Study | K_S (GPa) | K_T (GPa) | G (GPa) | $(\partial K_S/\partial P)_T$ | $(\partial K_T/\partial P)_T$ | $(\partial G/\partial P)_T$ |
|--|-------------|-------------|-----------|-------------------------------|-------------------------------|-----------------------------|
| This study ^a | 84.5 (5) | 82.0 (7) | 42.8 (2) | 4.78 (13) | 4.83 (13) | 1.08 (7) |
| Ultrasonic interferometry ^b | | | | | | |
| H | 83.9 (2) | | 43 (2) | | | |
| H-R | 84.70 (3) | | 43 (2) | 6.26 (18) | | 1.05 (7) |
| W-S | 83.1 | | 43 (2) | 4.92 | | 1.22 |
| B-V | 85.3 | | 43 (2) | 4.71 | | 1.18 |
| J | 84.5 (4) | | 43 (2) | | | |
| Average | 84.5 (6) | | 43 (2) | | | |
| Theory ^c | | | | | | |
| Ca | 82.6 | | | | | |
| MP | 82.7 | | | 4.0 | | |
| X-ray diffraction | | | | | | |
| A | | 81.02 (12) | | | 5.22(35) | |
| Brillouin spectroscopy | | | | | | |
| C | 81 (2) | | 44 (3) | | | |

^a K_S , G , and their pressure derivatives are from finite strain fits incorporating high-pressure data together with average values of the elastic constants under ambient conditions from ultrasonic interferometry. K_T and its pressure derivative are calculated from the isentropic moduli using thermodynamic identities (see text)

^b Previous studies: *H* Haussühl (1963); *H-R* Ho and Ruoff (1967); *W-S* Wong and Schuele (1968); *B-V* Brielles and Vidal (1975); *J* Jones (1977); *Ca* Catti et al. (1991); *MP* Martín-Pendás et al. (1994); *A* Angel (1993); *C* Catlow et al. (1978)

^c Athermal parameters

Fig. 1 Schematic diagram of the Brillouin scattering setup. DAC Diamond anvil cell; MCA multichannel analyzer

where λ_0 is the incident laser wavelength, and α is the external incidence angle. In all the measurements a 40° external incidence angle was used.

The precision, accuracy, and reproducibility of our Brillouin system were tested on platelets of MgO and MgAl₂O₄ at standard conditions. The precision of the single-crystal acoustic velocity measurements can be stated to 0.5% (at 1 σ level) in the velocity range between 5.3 and 9.8 km s⁻¹. The accuracy, tested on both longitudinal and transverse acoustic modes in directions on the (100) plane of MgO and (111) plane of MgAl₂O₄ and expressed as discrepancy with respect to the expected velocity, is always better than $\pm 0.75\%$. The reproducibility (misalignment or defocusing during the setup of the optic path outside the spectrometer) was always better than $\pm 0.5\%$ of the measured velocities in the range 5.3 to 9.8 km s⁻¹.

Raman scattering measurements

Single-crystal Raman spectra were measured to 49.2 GPa. A fragment derived from the same (111) crystal plate as that used for Brillouin scattering was loaded in a symmetric diamond anvil cell and compressed between two 300- μ m diamond culets with cryogenically loaded Ar as a pressure-transmitting medium. Ruby chips were loaded at different positions for pressure determination and to monitor the homogeneity of the stress conditions. Pressure differences never exceeded ± 1 GPa.

Raman scattering measurements were also performed on the same platelet used in the Brillouin experiment at 8.5, 8.9, and 9.3 GPa. Finally, Raman spectra of a polycrystalline CaF₂ sample loaded with a 4:1 volume mixture of methanol and ethanol as a pressure medium were measured to 11 GPa.

The Raman experiment was performed using a 200-mW Ar-ion laser ($\lambda = 514.532$ nm) as an excitation source. The optic setup of our system (Shim and Duffy 2002) is based on the use of holographic optics and on confocal imaging of the scattering region and follows the design outlined by Goncharov et al. (2000). The Raman signal was collected using a single-grating 0.5-m spectrometer and a 1100×330 -pixel CCD detector.

Results and discussion

Brillouin spectra were collected in 19 to 30 different crystallographic directions at each of 11 pressures between 1.0 and 9.3 GPa. The quasilongitudinal and both quasi-shear acoustic modes were detected. A representative spectrum is shown in Fig. 2. The dependence of acoustic velocities in CaF_2 as a function of direction in the (111) plane at a representative pressure is shown in Fig. 3.

The elastic tensor of fluorite is characterized by three independent elastic constants, C_{11} , C_{12} , and C_{44} . The acoustic velocity data and an initial density were inverted using a nonlinear least-squares fitting to the Christoffel equation, based on the Levenberg–Marquardt algorithm and the Cardano formulas (Every 1980), to obtain both the elastic constants and the phonon propagation direction. The elastic constants were determined to a precision of $\pm 1\%$ and the orientation to a precision of $\pm 1^\circ$. The overall accuracy of the inverted orientation, estimated as the standard deviation of the averaged orientation at the different pressures, is $\pm 2^\circ$, and it is affected by trade-offs with the elastic constants. The inverted constants allowed us to calculate the aggregate adiabatic bulk modulus and the Voigt–Reuss–Hill average (Hill 1963) of the aggregate shear modulus at each pressure.

Our inverted high-pressure moduli were combined with the average of selected published values for the individual constants and aggregate bulk and shear modulus of fluorite at ambient pressure for fitting to third-order finite strain equations (Birch 1978; Davies and Dziewonski 1975). The elastic moduli determined at standard conditions by Brillouin spectroscopy by Catlow et al. (1978) were not included in the average

because of the anomalously low value of C_{12} in this study for which few phonon directions were measured.

An iterative procedure was adopted to determine the finite strain parameters for the individual and aggregate elastic moduli (Davies and Dziewonski 1975; Birch 1978) as well as the density at each pressure. An initial density model was used to obtain the ambient-pressure values of the adiabatic bulk modulus, K_{0S} , and its first pressure derivative, $(\partial K_{0S}/\partial P)_T$ from a least-squares fit to the finite strain equation. These values were then corrected to the corresponding ambient-pressure isothermal values, $(K_{0T}, (\partial K_{0T}/\partial P)_T)$ using known values for various thermodynamic parameters (Table 4). These isothermal parameters were then used to construct the isothermal compression curve and obtain refined densities. The procedure was repeated until convergence. Fit results for individual moduli and their derivatives are listed in Table 1, while results for the aggregate moduli and their derivatives are listed in Table 2. The resultant densities at each pressure are given in Table 3.

It is notable that the isotherm derived from the Brillouin scattering data is independent of the initial density model with the exception of the density at zero pressure, fixed to our measured value. The inversion procedure converged to the final solution in six iterations when starting from an arbitrary initial density model, while it converged in three iterations starting from the Angel (1993) density scale. The root mean square differences between observed and calculated sound velocities and the best-fit values of the density and of the isentropic elastic constants at each pressure step are reported in Table 3.

The velocity anisotropy in the (111) plane, expressed as deviation of the longitudinal and the two transverse modes velocities from their average values, shows a decrease from 1.4, 13.0, and 10.8%, respectively, at 1.0 GPa to average values of 0.9 (± 0.2)%, 9.4 (± 0.4)%, 7.8 (± 0.3)% in the range 8.2–9.0 GPa. A significant increase of the longitudinal velocity anisotropy is observed at $P = 9.3$ GPa (from 0.9 to 1.2%). The elastic anisotropy of fluorite, expressed in the form $A^{-1}-1$ [where $A = 2C_{44}/(C_{11} - C_{12})$, Auld 1973], which

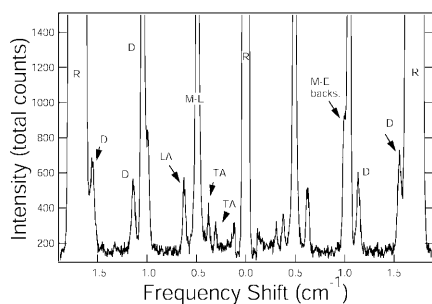


Fig. 2 Representative Brillouin spectrum of CaF_2 collected at 5.54 GPa. *LA* Quasi-longitudinal acoustic mode; *TA* quasitransverse acoustic modes; *M-E* peaks from methanol–ethanol in both forward and backscattering geometries; *D* diamond; *R* unshifted Rayleigh line

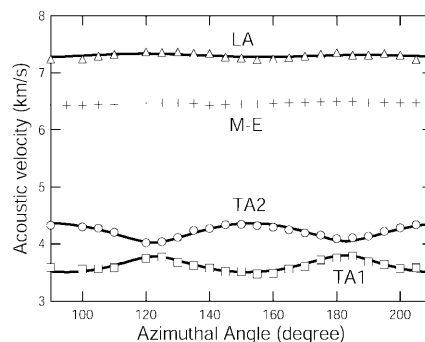


Fig. 3 Quasilongitudinal and quasitransverse acoustic velocities in the (111) plane of CaF_2 at 8.2 GPa as a function of crystallographic direction. The *azimuthal angle* is relative to an arbitrary starting direction. The *continuous curves* are calculated using the best-fit elastic constants. Abbreviations as in Fig. 2

Table 3 Density and elastic constants of CaF₂. Numbers in parentheses are one standard deviation uncertainty in the last digits

| Pressure (GPa) | ρ (Mg m ⁻³) | C_{11} (GPa) | C_{12} (GPa) | C_{44} (GPa) | RMS ^a (m s ⁻¹) | Pressure medium |
|----------------|------------------------------|----------------|----------------|----------------|---------------------------------------|------------------|
| 0.95 (5) | 3.222 (2) | 170.9 (7) | 47.5 (5) | 34.0 (6) | 39.6 | Si grease |
| 3.31 (5) | 3.306 (2) | 183.3 (3) | 60.0 (3) | 38.0 (1) | 40.6 | Si grease |
| 3.96 (5) | 3.328 (2) | 192.7 (4) | 62.0 (4) | 38.5 (2) | 38.4 | M-E ^b |
| 5.54 (5) | 3.378 (3) | 195.2 (4) | 67.2 (4) | 39.8 (1) | 31.7 | M-E |
| 6.65 (5) | 3.412 (2) | 201.5 (4) | 71.1 (4) | 41.4 (1) | 41.0 | M-E |
| 6.95 (5) | 3.422 (2) | 204.3 (4) | 73.2 (4) | 41.6 (1) | 37.8 | M-E |
| 7.48 (5) | 3.437 (2) | 206.4 (5) | 72.9 (6) | 43.5 (1) | 44.8 | M-E |
| 8.15 (5) | 3.457 (2) | 206.4 (5) | 74.8 (6) | 42.5 (1) | 30.9 | M-E |
| 8.35 (5) | 3.642 (2) | 209.5 (4) | 77.0 (4) | 42.2 (1) | 35.6 | M-E |
| 8.95 (5) | 3.480 (2) | 213.9 (5) | 81.8 (5) | 42.7 (1) | 41.1 | M-E |
| 9.31 (5) | 3.490 (2) | 220.2 (5) | 84.8 (5) | 43.2 (1) | 34.0 | M-E |

^a RMS: Root mean square difference between observed and calculated sound velocities

^b M-E: methanol-ethanol mixture

has a value of zero for an isotropic materials, decreases from 0.81 at 1.0 GPa to an average value of 0.56 ± 0.02 in the range 6.7–9.3 GPa.

The pressure dependence of the inverted elastic constants is shown in Fig. 4. The uncertainties on the constants, expressed as 1σ of the inverted value, are in the range of 0.5–1% at each pressure. Fits of C_{11} and C_{12} to third order Eulerian strain equations (Birch 1978) yield pressure derivatives of the adiabatic constants (Table 1) which are consistent with low-pressure ultrasonic data of Wong and Schuele (1968) and Brielles and Vidal (1975), but not with those of Ho and Ruoff (1967). Our results for $(\partial C_{44}/\partial P)_T$, are significantly lower (1.12) than the range of values (1.29–1.33) found in the earlier low-pressure studies. Shear ultrasound velocity measurements are sensitive to small misalignments of the transducer, with large effects on the uncertainty in C_{44} determination (Ho and Ruoff 1967). Furthermore, the small observed range for C_{44} in these studies contrasts with larger discrepancies in C_{11} and C_{12} , suggesting that the agreement may be fortuitous.

The fit values of the pressure derivatives of the isentropic bulk modulus and of the shear modulus are 4.78 ± 0.13 and 1.08 ± 0.07 , respectively. The value of the pressure derivative of the bulk modulus is again significantly smaller than the value obtained by Ho and Ruoff (1967) (because of their anomalous value for the pressure derivative of C_{12}) but in good agreement with those determined by Wong and Schuele (1968) and Brielles and Vidal (1975) (Table 2). The pressure derivative of the shear modulus from Brillouin scattering is, instead, in good agreement with the value calculated from the results of Ho and Ruoff (1967) but smaller than the values determined in the other ultrasonic interferometry studies (Table 2). The adoption of the pressure derivative of the bulk modulus from low-pressure ultrasonic elasticity measurements performed in small pressure range produces an isothermal equation of state sensibly different than that directly determined by Brillouin spectroscopy in this study. The results of Wong

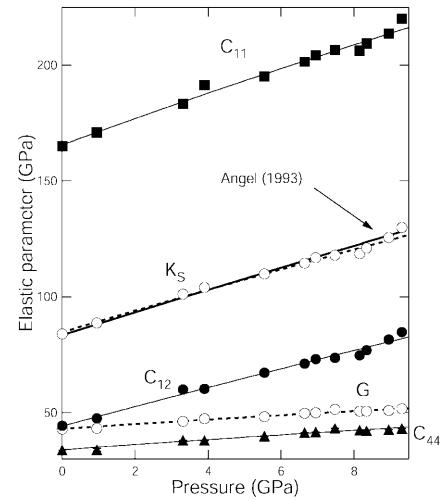


Fig. 4 Individual and aggregate Voigt–Reuss–Hill elastic moduli of CaF₂, as a function of pressure. The *continuous lines* are third-order Eulerian strain fits to the pressure dependence of the individual moduli. The isentropic bulk modulus and the shear modulus dependence on pressure (*dashed curves*) were determined by inversion of the experimental values of the moduli to third-order Eulerian strain equations (see text). The *solid curve* is the pressure dependence of the isentropic bulk modulus obtained by conversion from the Angel (1993) isothermal equation of state. It is plotted for comparison with the result of this study (the Reuss and Voigt bounds for the bulk modulus are equivalent in cubic materials)

and Schuele (1968) and Brielles and Vidal (1975) underestimate the bulk modulus by 0.3 and 0.7% at 9 GPa while Ho and Ruoff (1967) overestimate it by 3%. A possible explanation of these discrepancies is the complex pressure dependence of the transducer–bond phase shift, which can generate errors to 10% in the pressure derivatives of the elastic moduli determined by ultrasonic interferometry (Jackson et al. 1981; Weidner 1987).

The fit value of the adiabatic bulk modulus at standard conditions is 84.5 ± 0.5 GPa. The isothermal bulk modulus calculated applying the thermodynamic identity $K_{0T} = K_{0S}/(1 + \alpha\gamma T)$, where α is the volume thermal expansion coefficient and γ is the Grüneisen parameter (Table 4), yields 82.0 ± 0.7 GPa. This is in agreement within mutual uncertainties with the value of 81.0 ± 1.2 GPa determined by Angel (1993) from single-crystal X-ray diffraction measurements. The pressure derivative of the isothermal bulk modulus at standard conditions, calculated using the relation: $(\partial K_{0T}/\partial P)_T \cong (1 + \alpha\gamma T)^{-1} [(\partial K_{0S}/\partial P)_T - \gamma T/K_T (\partial K_{0T}/\partial T)_P]$ (see Table 4), is 4.83 ± 0.13 , which is consistent within reciprocal uncertainties with the value of 5.22 ± 0.35 reported by Angel (both bulk modulus and its pressure derivative reported in Angel 1993 are the results of a fit to the third-order Birch–Murnaghan equation and not to the Murnaghan equation, as erroneously stated in that paper; R. Angel, personal communication). The resulting 298 K isotherm is stiffer (due to a higher K_{0T}) at low pressure, with a maximum pressure difference ΔP of +0.04 GPa at $P = 3.7$ GPa; then it becomes softer because of the effect of the lower pressure derivative of

Table 4 Thermodynamic and thermoelastic parameters of CaF_2 under ambient conditions. ρ_0 Density at ambient conditions (Mg m^{-3}). T temperature (K)

| Parameter | | Reference |
|------------------------------------|--|---------------------------------------|
| Thermal expansion $T(\alpha_0)$ | $5.7 (7) \times 10^{-5} \text{ K}^{-1}$ | Schumann and Neumann (1984) |
| Specific heat (C_P) | $87.85 \text{ J kg}^{-1} \text{ K}^{-1}$ | Chase (1998) |
| Grüneisen parameter (γ_0) | 1.74 (21) | Calculated ^a |
| $(\partial K_{0S}/\partial T)_P$ | $-0.021 (1) \text{ GPa K}^{-1}$ | Wong and Schuele (1968); Jones (1977) |
| $(\partial K_{0T}/\partial T)_P$ | $-0.031 (2) \text{ GPa K}^{-1}$ | Calculated ^b |

^a Grüneisen parameter obtained as: $\gamma_0 = \alpha_0 K_S / (\rho_0 C_P)$

^b Calculated as: $(\partial K_T/\partial T)_P \equiv (\partial K_S/\partial T)_P / (1 + \alpha\gamma T) - K_S / (1 + \alpha\gamma T)^2 [\alpha\gamma + (\partial\alpha/\partial T)\gamma T]$

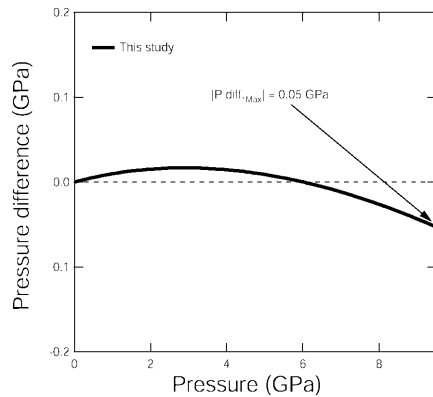


Fig. 5 Difference between isothermal equation of state determined in this Brillouin scattering study and the isotherm determined by Angel (1993) based on X-ray diffraction experiments

the bulk modulus, with a maximum difference ΔP of -0.03 GPa at 9.5 GPa (Fig. 5).

Poisson's ratio for an isotropic polycrystalline aggregate of fluorite, calculated using the aggregate moduli from our measured single-crystal elastic constants, increases from 0.29 at 1.0 GPa to 0.32 at 9.3 GPa . The Cauchy relation $C_{12} = C_{44}$ (Born and Huang 1954), and its generalization for hydrostatic pressure, $C_{12} = C_{44} + 2P$ (Korpiun and Lüscher 1976), are not satisfied by fluorite. The violation of the Cauchy relation increases from 12 to 23 GPa in the investigated pressure range. The violation of the Cauchy relation indicates that a simple central force model (e.g., Anderson and Demarest 1971) is not able to describe the elastic properties of fluorite. Theoretical investigations of CaF_2 by means of ab-initio (Catti et al. 1991) and combined first-principles and ab-initio techniques (Martín-Pendás et al. 1994) produced values of the bulk modulus at 0 K of 82.6 and 82.7 GPa, respectively, which are in reasonable agreement with the value determined in our study, but the values of the single constants are in substantial disagreement with the experimental results (Table 1). The pressure dependence of both the bulk modulus and the individual elastic constants reported by Martín-Pendás et al. (1994) are substantially underestimated compared with experimental results (Tables 1, 2).

A detailed analysis of our measurements suggests a variation in the behavior of CaF_2 at $P \geq 9.0 \text{ GPa}$, which affects the pressure dependence of the elastic moduli.

Weakening of the X-ray diffraction peaks was observed in the same pressure range by Angel (1993) in single-crystal experiments. This anomalous behavior could be related to the structural phase transition to an orthorhombic phase (PbCl_2 structure type) reported at 9.5 GPa (Seifert 1966; Gerward et al. 1992). The twinning associated with the transformation (see Angel 1993) precludes the possibility of reliable Brillouin scattering measurements of the high-pressure phase. Raman scattering of the platelet used for Brillouin scattering revealed the presence of new weak features related to the high-pressure phase at $P = 9.3 \text{ GPa}$. We performed Raman measurements of a different platelet from the same sample used in the Brillouin experiments, in the range 0–49.2 GPa. The single Raman-active mode of the cubic phase of CaF_2 was observed in the stability field of fluorite. It showed a linear pressure dependence of the frequency shift given by: $\partial\nu/\partial P = 4.93 \text{ cm}^{-1} \text{ GPa}^{-1}$. The onset of the transition is characterized by the appearance of the 18 active Raman modes characteristic of the orthorhombic PbCl_2 type structure (Mendes-Filho et al. 1979). We were able to identify seven Raman features (Fig. 6) in the 160 to 440 cm^{-1} frequency range that were observed up to 50 GPa (Fig. 6, 7). The first appearance of the new features in this experiment was at $P = 8.7 \text{ GPa}$. No remnants of the single Raman-active mode of the cubic phase were detected at $P \geq 11 \text{ GPa}$. The high-pressure phase was observed metastably to $P > 7 \text{ GPa}$ during decompression. The cubic fluorite Raman mode reappeared at $P \leq 8 \text{ GPa}$. Raman scattering to 11 GPa of a polycrystalline CaF_2 sample showed the same behavior in compression as the single-crystal samples; however the Raman modes of the high-pressure phase were observed upon decompression to 4 GPa . This body of observations suggests that the degree of hysteresis is affected by the detail of the compression history and the microstructure of the sample. The appearance of a Raman signal from phonon modes of the orthorhombic high-pressure phase in the 8.7- to 9.5- GPa pressure range suggests that the local instabilities related to the nucleation of the high-pressure phase have a short wavelength compatible with the Raman effect but they do not completely break the overall cubic symmetry at the scale of hundreds of unit cells probed by Brillouin scattering, where they generate a subtle nonlinearity of the pressure dependence of the quasilongitudinal velocities, and they are smeared out in average by the large volume probed

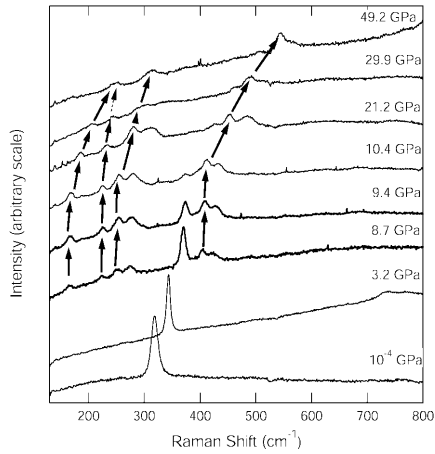


Fig. 6 Representative Raman spectra of the cubic low-pressure phase and the orthorhombic high-pressure phase of CaF_2 to 49.2 GPa. Pressures are listed next to each spectrum

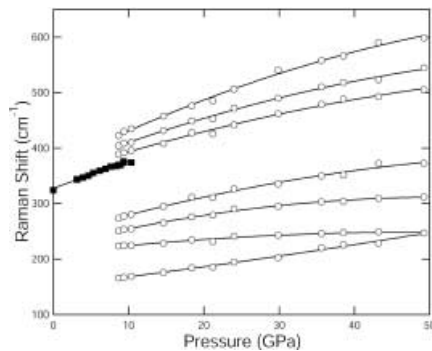


Fig. 7 Pressure-induced frequency shift of phonon modes of the low-pressure cubic phase (solid squares) and of the high-pressure orthorhombic polymorph of CaF_2 in the 150–800 cm^{-1} frequency range to 49.2 GPa. All the data were obtained on a single crystal with increasing pressure

by X-ray diffraction experiments, where they generate a weakening and broadening of the diffraction peaks. Inverting only the Brillouin data clearly unaffected by visible traces of structural instabilities to 9 GPa does not yield any significant change in the aggregate moduli or their pressure derivatives.

Summary

Brillouin spectra measured to 9.3 GPa at 300 K allow us to better characterize the high-pressure elasticity of calcium fluoride. The pressure derivative of the isothermal bulk modulus determined in this study is 8% lower and more precise by a factor of 3 than that obtained from static compression data (Angel 1993). This difference is partially explained by the correlation between bulk modulus and its pressure derivative in the inversion of X-ray diffraction data and also by the relatively small pressure stability range of fluorite. It is

notable that the inverted bulk modulus of Angel (1993) is 2% lower than the isothermal bulk modulus determined in this study.

Our results extend the pressure range of direct measurements of the elasticity of fluorite by nearly 1 order of magnitude with respect to previous ultrasonic data. Low-pressure ultrasonic studies of Wong and Schuele (1968) and Brielles and Vidal (1975) underestimate the bulk modulus by 0.3 and 0.7% at 9 GPa, while Ho and Ruoff (1967) overestimate it by 3%. The disagreements between our pressure derivative of the shear modulus with respect to Wong and Schuele (1968) and Brielles and Vidal (1975) are almost entirely explained by the difference in the pressure derivative of C_{44} , which is smaller in our Brillouin measurements. However, it is important to note that the discrepancies between the three available high-pressure ultrasonic datasets are as large as the discrepancy with respect to our results. It has been previously observed that low-pressure ultrasonic studies tend to systematically overestimate pressure derivatives when compared with direct high-pressure measurements (e.g., Zha et al. 1996).

This study confirms that Brillouin spectroscopy of minerals of cubic symmetry allows the simultaneous recovery of elastic moduli, orientation, and density, in agreement with previous results for MgO (Sinogeikin and Bass 2000). The new high-pressure elasticity dataset allowed us to determine a new independent isothermal equation of state for fluorite, which agrees with that of Angel (1993) to better than 1%, providing a strong confirmation of the fluorite pressure scale from 0 to 9 GPa.

Acknowledgements We thank Ross Angel and an anonymous reviewer for their detailed comments, which allowed us to improve the manuscript and clarify some critical aspects of the discussion. We also thank C.-S. Zha for his valuable technical assistance and S. Shieh and S.-H. Shim for their comments and suggestions.

References

- Anderson OL, Demarest HH (1971) Elastic constants of the central force model for cubic structures: polycrystalline aggregates and instabilities. *J Geophys Res* 76: 1349–1369
- Angel RJ (1993) The high-pressure, high-temperature equation of state calcium fluoride, CaF_2 . *J Phys Condens Matter* 5: L141–L144
- Angel RJ, Allan DR, Miletich R, Finger LW (1997) The use of quartz as an internal pressure standard in high-pressure crystallography. *J Appl Crystallogr* 30: 461–466
- Barnett JD, Block S, Piermarini GJ (1973) An optical fluorescence system for quantitative pressure measurement in the diamond-anvil cell. *Rev Sci Instr* 44: 1–9
- Birch F (1978) Finite strain isotherm and velocities for single-crystal and polycrystalline NaCl at high pressures and 300 K. *J Geophys Res* 83: 1257–1268
- Born M, Huang K (1954) *Dynamical theory of crystal lattices*. Clarendon Press, Oxford, 420 pp
- Brielles J, Vidal D (1975) Variation des constantes élastiques de la fluorine CaF_2 avec la pression jusqu'à 12 kbar. *High Temp-High Pressures* 7: 29–33

- Catlow CRA, Comins JD, Germano FA, Harley RT, Hayes W (1978) Brillouin scattering and theoretical studies of high-temperature disorder in fluorite crystals. *J Phys (C)* 11: 3197–3212
- Catti M, Dovesi R, Pavese A, Saunders VR (1991) Elastic and electronic structure of fluorite (CaF_2): an ab-initio Hartree-Fock study. *J Phys Condens Matter* 3: 4151–4164
- Chai M, Brown MJ (1996) Effects of static non-hydrostatic stress on the R lines of ruby. *Geophys Res Lett* 23: 3539–3542
- Chase MJ, Jr (1998) NIST-JANAF thermochemical tables, 4th ed. *J Phys Chem Ref Data Monograph* no. 9, American Chemical Society, New York, American Institute of Physics for the National Institute of Standards and Technology, pp. 716–719
- Dandekar DP, Jamieson JC (1969) Some high-pressure phases of RX_2 fluorides. *Trans Am Crystallogr Ass* 5: 19–27
- Davies GF, Dziewonski AM (1975) Homogeneity and constitution of the Earth's lower mantle and outer core. *Phys Earth Planet Int* 10: 336–343
- Every AG (1980) General closed-form expressions for acoustic waves in elastically anisotropic solids. *Phys Rev (B)* 22: 1746–1760
- Gerward L, Staun Olsen J, Steenstrup S (1992) X-ray diffraction of CaF_2 at high pressure. *J Appl Crystallogr* 25: 578–581
- Goncharov AF, Struzhkin VV, Hemley RJ, Mao H-K, Liu Z (2000) New techniques for optical spectroscopy at ultrahigh pressures. In: Manghnani MH, Nellis WJ, Nicol MF (eds) *Science and technology of high pressure*. University Press, India, pp 90–95
- Haussühl S (1963) Das elastische Verhalten von Flussspat und strukturverwandten Kristallen. *Phys Stat Solid* 3: 1072–1076
- Hazen RM, Finger LW (1981) Calcium fluoride as an internal pressure standard in high-pressure/high-temperature crystallography. *J Appl Crystallogr* 14: 234–236
- Hill R (1963) Elastic properties of reinforced solids: some theoretical principles. *J Mech Phys Solids* 11: 357–372
- Ho PS, Ruoff AL (1967) Pressure dependence of the elastic constants and an experimental equation of state for CaF_2 . *Phys Rev* 161: 864–869
- Jackson I, Niesler H, Weidner DJ (1981) Explicit correction of ultrasonically determined elastic wave velocities for transducer-bond phase shifts. *J Geophys Res* 86: 3736–3748
- Jones LEA (1977) High-temperature elasticity of the fluorite-structure compounds CaF_2 , SrF_2 , and BaF_2 . *Phys Earth Planet Int* 15: 77–79
- Katrusiak A, Nelmes RJ (1977) A test of the accuracy of high-pressure measurements using a Merrill-Bassett diamond-anvil cell. *J Appl Crystallogr* 19: 73–76
- Korpiun P, Lüscher E (1976) Thermal and elastic properties at low pressure. In: Venables JA, Klein ML (eds) *Rare gas solids*. Academic press, New York, vol. 2, p 729
- Léger JM, Haines J, Atouf A, Schulte O, Hull S (1995) High-pressure X-ray and neutron diffraction studies of BaF_2 : an example of a coordination number of 11 in AX_2 compounds. *Phys Rev (B)* 52: 13247–13256
- Lindsay SM, Anderson MW, Sandercock JR (1981) Construction and alignment of a high-performance multipass Vernier tandem Fabry-Perot interferometer. *Rev Sci Instrum* 52: 1478–1486
- Mao HK, Xu J, Bell PM (1986) Calibration of the ruby pressure gauge to 800 kbar under quasi-hydrostatic conditions. *J Geophys Res* 91: 4673–4677
- Martín-Pendás A, Recio JM, Flrez M, Luaña V (1994) Static simulation of CaF_2 polymorphs. *Phys Rev (B)*, 49: 5858–5868
- Mendes-Filho J, Melo FEA, Moreira JÉ (1979) Raman spectra of lead chloride single crystal. *J Raman Spectros* 8: 199–202
- Merrill L, Bassett WA (1974) Miniature diamond-anvil pressure cell for single-crystal X-ray diffraction studies. *Rev Sci Instrum* 45: 290–294
- Miletich R, Allan DR, Kuhs WF (2001) High-pressure single-crystal techniques. In: Hazen RM, Downs RT (eds) *High-temperature and high-pressure crystal chemistry*. Reviews in Mineralogy and Geochemistry, vol. 41, Mineralogical society of America, Washington DC, pp. 445–519
- Morris E, Groy T, Leineweber K (2001) Crystal structure and bonding in the high-pressure form of fluorite (CaF_2). *J Phys Chem Solids* 62: 1117–1122
- Schumann B, Neumann H (1984) Thermal expansion of CaF_2 from 298 to 1173 K. *Crystal Res and Technol* 19: K13–K14
- Seifert K-F (1966) Strukturumwandlungen von Halogeniden des Typus AX_2 unter höheren Drücken. *Ber Bunsenges Phys Chem* 70: 1041–1042
- Shim S-H, Duffy TS (2002) Raman spectroscopy of Fe_2O_3 to 62 GPa. *Am Mineral* 87: 318–326
- Sinogeikin SV, Bass JD (2000) Single-crystal elasticity of pyrope and MgO to 20 Gpa. *Phys Earth Planet Inter* 120: 43–62
- Vidal D (1974) Measurements of elastic constants of single crystal calcium-fluoride between 20° and 850 °C. *CR Sci, Ser B*, 279 (14): 345–347
- Weidner DJ (1987) Elastic properties of rocks and minerals. In: Summis CG, Henyey TL (eds) *Methods of experimental physics*, Academic Press, New York, Vol. 24A. pp 1–30
- Withfield CH, Brody EM, Bassett WA (1976) Elastic moduli of NaCl by Brillouin scattering at high pressure in a diamond-anvil cell. *Rev Sci Instrum* 47: 942–947
- Wong C, Schuele DE (1968) Pressure and temperature derivatives of the elastic constants of CaF_2 and BaF_2 . *J Phys Chem Solids* 29: 1309–1330
- Zha C-S, Duffy TS, Downs RT, Mao H-K, Hemley RJ (1996) Sound velocity and elasticity of single-crystal forsterite to 16 Gpa. *J Geophys Res* 101: 17535–17545